Light Absorption Near Infrared Wavelength by Laser Pulsed Texturing on Multi-crystalline Silicon Solar Cells

Nurfarizza Surhada Mohd Nasir
Solar Energy Research Institute, Universiti Kebangsaan Malaysia
nasir989surhada@gmail.com

Suhaila Sepeai
Solar Energy Research Institute, Universiti Kebangsaan Malaysia
suhailas@ukm.edu.my

Mohd Adib Ibrahim
Solar Energy Research Institute, Universiti Kebangsaan Malaysia
mdadib@ukm.edu.my

Kamaruzzaman Sopian
Solar Energy Research Institute, Universiti Kebangsaan Malaysia
ksopian@ukm.edu.my

Abstract

In the photovoltaic (PV) sector, thin silicon (Si) wafers in multi-crystalline (mc-Si) silicon solar cells offer an option for cost-effectiveness. When the thickness of Si solar cells is less than 100 µm, however, optical loss becomes a critical factor. The silicon bandgap on the other hand is critical in the long-wavelength range of 900 to 1200 nm. As a result, it is captious to look at how to improve the cell conversion efficiency at long wavelengths. In this paper, we were able to design and fabricate deeply etched micro-textured structure (DELMS) silicon solar cells using pulsed laser radiation. On the front surface of multi-crystalline Si solar cells, the pulsed laser energy power ranged from 15.2W (E1), 23.5W (E2), and 32.5W (E3). With specific depths, widths, and diameters of patterns applied, it boosted the internal scattering inside the sidewall of the structure of the solar cell. The infrared transmission response clearly shows that the DELMS improved the optical performance of cells in the longer wavelength. Our best samples. The short-circuit-current density, voltage open-circuit, and absolute efficiency present the improvement of ΔJ_{sc}= 0.5, ΔV_{oc}=1.83, and $\Delta\eta$=0.6%, respectively. The DELMS with 23.5W laser power exhibit an excellent 60.0% reduction in infrared (IR) transmission response compared with 15.2W, 32.5W, and pyramid texture.

Keywords: Laser-pulsed, Infrared, Light Absorption

1.0 Introduction

Significant cost savings are possible to the cost-effective utilization of crystalline silicon (c-Si) and the reduction of Si wafer thickness. These are caused by an indirect bandgap of Si was low infrared (IR) absorption near the band gap. The structure's scale was also constrained by the wafer thickness limits. Reduced c-Si wafer thickness, on the other hand, results in lower solar cell efficiency. To equivalence the thickness and efficiency, a variety of advanced light trapping schemes have been studied, including introducing nano-photonic structures (J. Baohua, 2015), random nanostructures (Amalathas & Alkaisi, 2019), periodic nanostructures (X. Li & Y. Gua, 2020), and metal nanoparticles (Zhou et al., 2017).

Recombination losses were lowered when the thickness of polycrystalline Si wafers was reduced (Zhou et al., 2017), and bigger open-circuit voltages resulted in significant optical absorption (Liu et al, 2020). By introducing scattering at rough interfaces or coupling of events to waveguide modes in the solar cell's absorber layers. The optical path length was greatly increased (Hüpkes et al., 2019). Through light trapping, light dispersion at the rough surface of the Si wafer increased light absorption within the intrinsic layer. As a result, great emphasis should be placed on improving light absorption near the IR wavelength and lowering device front reflection.

We note that, the form of textured morphology on both the front and rear surfaces of solar cells, with the former being advantageous for light in-coupling for light trapping. The visible and near IR light is absorbed by silicon solar cells as solar energy falls on the cell structure. Known that the photons in the red and near-infrared spectra work best for Si. Silicon's energy bandgap is 1.12eV, which means that photons with higher energy than Si's bandgap can cause the atoms and electrons to gain kinetic energy. However, extra photon energy beyond the Si bandgap is converted to heat.

Jeewandaran (2020) discovered that low-cost flexible optoelectronics and photovoltaic (PV) cells can operate at room temperature (RT) under near IR wavelength. Furthermore, photodetectors that can detect the short-wavelength IR spectral spectrum from 1300 to 2000 nm are in high demand. Nano-texturing on the top end of Si solar cells is generally thought to be an effective design for enhancing the anti-reflecting coating (ARC) effect and overcoming low near-IR absorption in c-Si solar cells [9]. Wet-texturing, which includes acidic etching and alkaline etching, is mostly utilized in conventional industries.

Nonetheless, the inefficient wet-texturing procedure not only wastes a lot of Si but also cannot reduce the surface reflectance of multi-crystalline Silicon (mc-Si) enough due to its different crystal orientations (Chen at al., 2017) Several different fabrication methods and technologies, such as laser texturing (Mutlak, Ahmed, Nayef, Al-zaidi, & Abdulridha, 2021), mechanical grooving texturing (Nadi, Bittkan, Lentz, Ding, & Rau, 2021), and ion etching (RIE) texturing, have been updated in recent years to texture the mc-Si wafers (Ngwe Zin, 2017). Different types of lasers are being used in a number of materials processing applications in the field.

Lasers have the advantage of non-contact processing and are already well established in industrial solar cell processes such as edge isolation (Otaegi et al., 2017), doping process (Park, Choi, Jang, Bae, & Lim, 2020) selective emitter formation (Weber, Gutscher, Lohmüller, Lohmüller & Brand, 2018) and laser texturing (Ali at al., 2018). As a result, we discovered that laser texturing may be used to generate a sub-micron scale on the surface of mc-Si wafers, lowering surface reflectance and increasing the light path without causing considerable damage. The process parameters include laser intensity and etching time in an alkaline solution, which are reasonably easy to manage in laser texturing. The alkaline chemical etches (100) planes and stops on (111) planes resulting in pyramids on the Si wafer surface that are typically 5 to 10-µm height and are randomly scattered across the surface of the c-Si wafer (Yilbas, Keles & Toprakli, 2017). Strong anisotropic alkaline-based chemical solutions enable the formation of textured surfaces with a 14.65 weighted reflection (Radfar, Nasser, Aldemir, Bele & Turan, 2018).

In this paper, we investigate the IR absorption enhancement on mc-Si by using a pulsed laser to form the DELMS that allows a longer light path length to travel inside the cell structure. The objective of this work was to study the performance of mc-Si solar cells with different laser power and comparable with pyramid texture. Moreover, pulsed laser processing has been chosen due to less heterogeneous illumination and less step temperature gradient (Andreani, Bozzola, Kowalczewski, Liscidini & Redorici, 2019) and fewer materials used or additional procedures. On the other hand, pulsed laser processing has the ability to reduce surface reflectance following random texturing introduced through melting, ablation, and recrystallization (Chong, Wilson, Mokkapati & Catchpole, 2012). Therefore, in this paper, the development and analysis of deeply etched laser microtextured (DELM) on multi-crystalline will be presented. The analysis of DELM by scanning electron microscope (SEM), microscope camera, and infrared transmission response. Those data and results provide a characterization of preminelary data that will determine the capability of DELM in allow light to transmit, reflect, refract, or be absorbed to the near region based on the area thickness developed by pulsed laser interactions. The author suggests adding on the post-texturing to modify the pattern texture on mc-Si to improve the light conversion efficiency of solar cells.

2.0 Literature Review

Nowadays, light trapping is one of the main topics in crystalline silicon solar cells and concerns most Si solar cell designs. Generally, light trapping deals with preventing the light that falls to the solar cell surfaces from leaving it again and thus enhancing the percentage of being absorbed inside the cell. [20] mentioned that silicon solar cells that have a thickness significantly greater than the wavelength, could be used to provide perfect randomization of the light direction and optimal light trapping. Many approaches have been proposed to enhance the absorption in the long wavelength range (Chong, Wilson, Mokkapati & Catchpole, 2012) such as increasing the collection efficiency through randomly roughened surfaces and light trapping by optical structures (Ning et al., 2007) agreed that optical nanostructures reveal great potential in this field.

This newly proposed method is not only increasing the optical characteristics but can increase the efficiency of solar cells. The originality of this structure is formed from the combination of the physical method (laser texturing) and the chemical method (post-texturing). The laser texturing uses a focused light that allows surface modification with structuring parameters without needing any mask. The structure parameters include laser power use, different depth, different shapes/patterns/features, or different widths (line/dot/column). Consequently, the Si surface becomes too rough after the laser-texturing, thus, a post-texturing process is needed to eliminate and modified the Si surface to become smoother so that reduce the sharp edges and recombination then improved the minority carrier at the cell structure (Radfar, Es & Turan, 2020)

The DELMS not only has a texture on the wafer surface but it also creates the pyramidically texture inside the DELMS structure. Meaning that these features have an extra texture that will boost the light travel inside the cell. Rohaizar et al.(2019) mentioned that the surface texture on the front, rear, and sidewalls texture (features that form from the laser treatment process) contributes to enhancing the internal light scattering of the three-dimensional texturing. Therefore, the formation of pyramidically on the front and the rear side of the cell can reduce the reflection. Moreover, the light trapping scheme inside the solar cell either in the front or at the rear side will improve the optical path length, thus the electron-hole pair also will increase. Because of the changing the angle of incident of light rather than perpendicular to the wafer surface.

However, the major obstacles need to be realized that after the laser is aimed at the surface of the silicon wafer, not only generates the sludge, slag, or residue but, will form a texture depending on the laser power used. And how depth and width need to be optimized so as will boost the light trapping inside the cell. Fujishima et al. (2010) reported that the V_{oc} almost increased, whereas the J_{sc} gradually decreased when the wafer thickness decreased to less than 100 μm owing to the substantial loss in light absorption. On the other hand, Abott (2006) described that a lot of defects such as dislocation and silicon slag were formed in the laser-induced crater array, resulting in the decrease of the open-circuit voltage V_{oc} of solar cells. In addition, Ding et al. (2020) explained that the previous study on laser texturing mainly focused on either the laser processing to form the crater arrays with low reflectance or the optimization of chemical etching for less recombination. The trade-off between reflectance and recombination must be considered by controlling the laser and etching process to achieve a higher conversion efficiency of solar cells.

Difficulty in removing the residual slags could be one of the problems that degrade the electrical performance. Meanwhile, Radfar et al. (2020) claimed that for mc-Si texturing process with the anisotropic etchant (KOH, NaOH) solutions is not practical due to the random crystallographic grains on the wafer surfaces. The use of an anisotropic acidic solution like HF/HNO3mixture for texturing mc-Si wafers leads to high efficiency by improving the light absorption in cell structure. However, Kim et al. [28]explained that HF is extremely toxic and the etching has a high operating cost. Thus, an alternative process for texturing using an alkaline solution could be safe and very economical. Regrettably, the alkaline etching is not effective in chemical reactions compared to the acidic HF etching solution.

The fact is that HF etching reduces reflection losses on wafer surfaces more effectively rather than alkaline etching (Zou et al., 2017). Meanwhile, Dobrzański & Drygała, (2008) described that the difference in reduction in reflectance between acidic HF etching and alkaline etching is sustainably diminished after deposition of anti-reflection coating and encapsulation during solar cell manufacturing (Dobrzański & Drygała, 2008). In addition, the performance ratios for alkaline and acidic textured poly-cells have only very small differences in texture structure on the wafer surfaces. Subsequently, as long as the alkaline textured cells provide an almost equivalent electrical performance to the acidic textured cells, it is attractive to employ the alkaline anisotropic etching when laser texturing is applied (Kim, Ha, Park & Kim, 2018).

3.0 Experimental Setup

The design of the deeply etched laser micro-textured structure (DELMS) silicon solar cells was made to maximize the light absorption in IR wavelength and increase the light to travel longer inside the sidewall of the structure of the solar cell Figure 1 shows the process flow diagram for laser-pulsed production of DELMS.

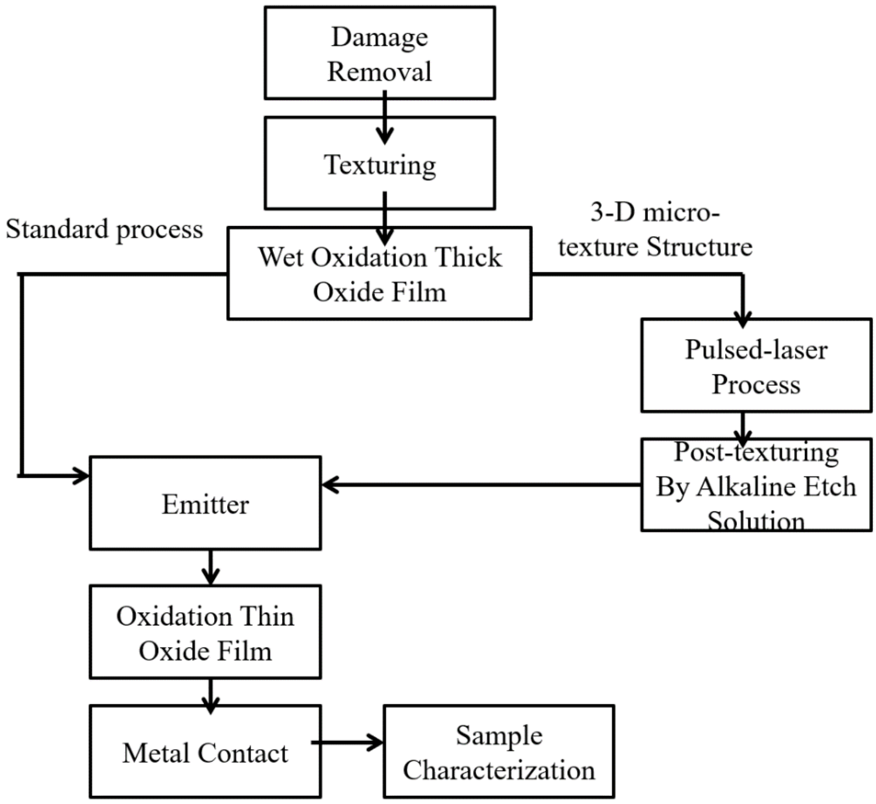

Figure 1: Processing steps in pulsed laser texture and alkaline etching to form deeply-etched three dimensional microstructure.

We employed 10 mm×10 mm, 200-µm thick, 100> orientated, p-type polycrystalline Si wafers with bulk resistivity in the range of 1 to 3-Ω.cm. The cleaning and saw damage removal (SDR) were accomplished by etching the as-cut wafers in 10.0% NaOH at 70°C for 15 minutes, followed by a deionized water (DI) rinse and removal of native oxide in dilute HF solution (HF:H_2O:1:5) to generate a hydrophobic surface. The wafer surface was then texturized at 70°C for 30 minutes in a (KOH:IPA:H_2O); (1:5:125) solution, followed by a DI water rinse. The thickness of the wafer after the cleaning and texturing is reduced by about 10% to 15% shown in Figure 2 which is 180 to 190-µm. The formation of DELM, thermal oxidation process was carried out prior to pulsed laser texturing. The oxidation was grown in an oxidation furnace at 1100 °C for 1 hour 30 minutes in oxygen ambient. The oxidation film act as a mask to protect the area without laser-induced so that this area will not be teched during the post-texturing process. The pulsed laser etching was carried out with six different powers (15.2 W, 23.5 W, 32.5W, 39.6 W, 44.8 W, and 47.0 W) under a 15 kHz pulse frequency.

The machine used to form the DELM was a part of the semiconductor laser dicing system (YMS-50D). The laser emits at a near-infrared (IR) invisible light beam with 1064 nm was chosen due to weak absorption and long penetration depth to facilitate the formation of vertically-etched through wide (Ning et al., 2007). However, with its long micro-second pulse duration laser interaction allows thermal-like molten deposition and heat-affected zone (HAZ) at the edge (Radfar, Es & Turan, 2020). Therefore, by applying the post-texturing process in 10% KOH solution at a temperature of 70 °C for an etching time of 120 minutes, it formed the DELM with different depths and width sizes due to different power on the front of the Si wafer surface. The pulsed laser is based on the CNC motion control software that controls MPC02 two-axis translation stage which is an x-y axis. The term CNC refers to machines that has program commands executed within the control. A CNC command in which commonly through a program tells the drive motor to rotate a precise number of times.

Figure 2: MD400E digital microscope picture after damage removal and texturing process with IPA: KOH:H_2O

3.1 DELMS Formation

Thermally produced silicon dioxide films were formed in a quartz furnace at 1100°C for 90minutes, using a laser etch mask of rough 350 nm thick thermally grown oxide. Following that, a polycrystalline Si wafer was treated with a pulsed laser beam with a diameter of 0.05mm and a separation distance of 1mm, as shown in figure 3. In figure 4, figure A shows the silicon surface before the DELM form. Meanwhile, the B, C, and D illustrate laser power employed at the defocus point was 15.2W, 23.5W, and 32.5W, respectively. This Figure to explain how the laser impact on the wafer surface with different power formed the different depths. The laser irradiating spot basically starts from the left-hand side to the right-hand side on the surface. We used the post-texturing technique because the surface roughness after the laser treatment was high, and it was necessary to remove the laser ablation residue or any materials due to the high temperature on the Si wafer caused by the absorption of laser energy. As presented in figure 5. the Si wafer with a laser pattern on the front surface was etched by dipping the sample in KOH solution at 70°C for 120minutes. However, some of the evacuated molten resolidified on the Si surface resulting in irregular particles in the hole-shaped.

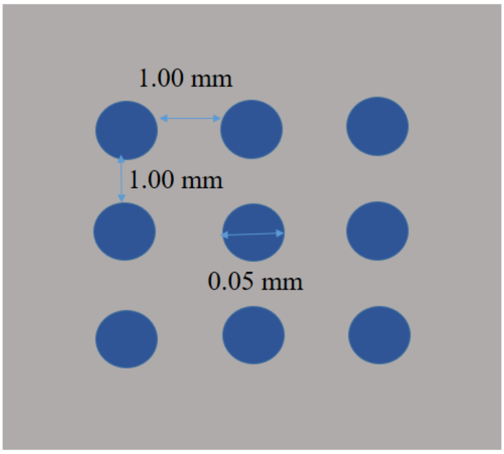

Figure 3: The schematic diagram for pulsed laser beam diameter of 0.05 mm and separation distance of 1mm, were treated on a polycrystalline Si wafer.

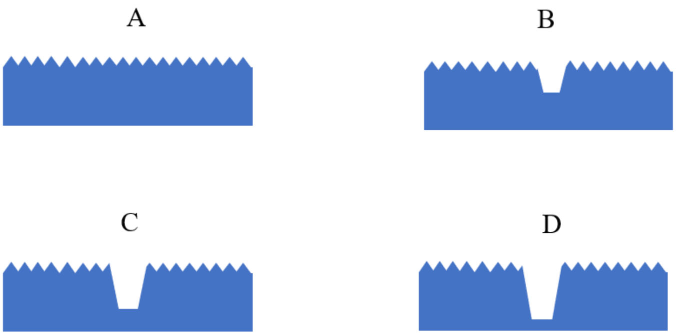

Figure 4: The illustration (a) before laser treatment and (b)15.2 W, (c) 25.2 W, and (d) 32.5 W after laser treatment of depth microstructure from three different power

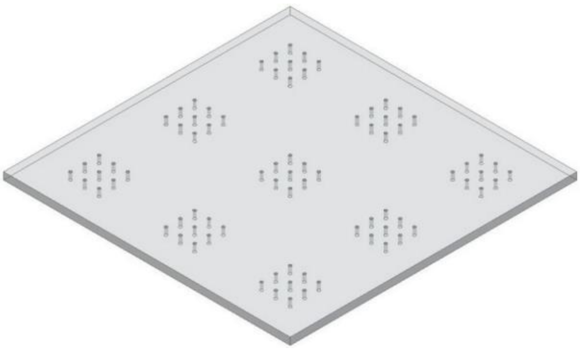

Figure 5: Schematic diagram of three-dimensional laser textures after deep into post-texturing with KOH etch solution.

3.2 DELMS Silicon Solar Cells

To generate the pattern for emitter deposition, we rinsed the sample in DI water and then exposed them to HF vapor for 30 s. The parameters for an emitter film deposited on a Si wafer are shown in Table 1. Using Dr. Blade's method with 10.0% phosphoric acid, the samples were annealed for 30 minutes in a quartz tube furnace at 875°C. After that, thermally generated silicon dioxide films were developed as an anti-reflection coating (ARC) layer on the surface of the wafer.

Table 1: Polycrystalline Si samples with a diameter of 0.05mm corresponding to laser power of 15.2W, 23.5W, and 32.5W, respectively compared to the polycrystalline Si wafer as a control substrate

Wafer poly/crystalline	Laser Power (W)	Average ohm/square	Standard deviation	Percentage variation
Pyramid textured (without 3-D texturing)	-	40.76	±3.84	24.73
Sample 1	15.2	40.08	±0.93	6.65
Sample 2	23.5	41.57	±0.90	6.65
Sample 3	32.5	41.28	±0.91	6.65

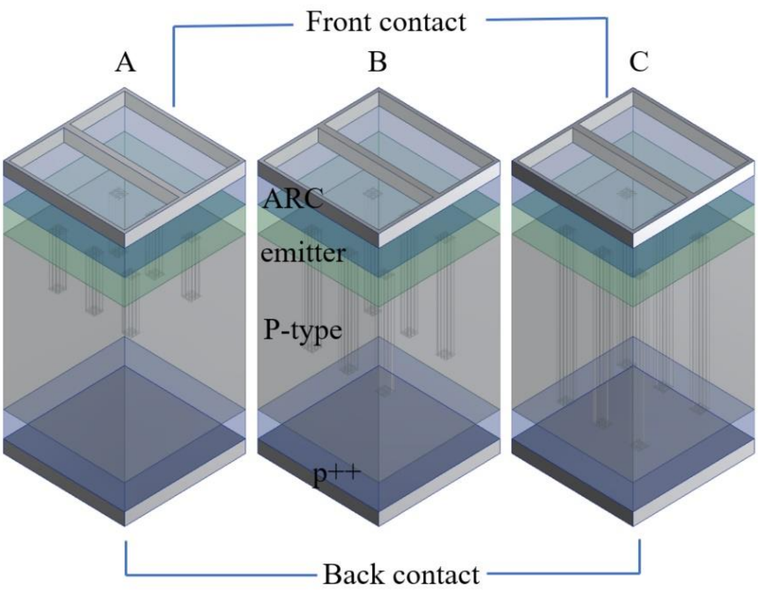

Figure 6: Schematic cross-section of polycrystalline Si solar cell with 3-dimensional microstructure at different etch

The front phosphorus-diffused side was screen-printed with Ag paste (SOL 9610A), while the non-diffused backside was screen-printed wafers were then dried for 15 minutes at 150°C in a thermal oven before being co-fired in a typical 6-zone conveyor belt infrared (IR) furnace (S-615C) as a function of the peak zone 4 temperature, while the temperatures in other five zones were kept constant. Finally, we laser-diced the samples into 1.5cm×1.5cm for light current-voltage (LIV) measurement as shown in figure 6.

There are three main characterization processes that were investigated for the optical analysis, Hitachi Field Emission Scanning Electron Microscopy (FESEM) was employed. SEM images provide the necessary information in order to determine the surface texture, depths, and width of the DELM structure. Figure 7 shows a schematic diagram for the microscope camera experimental setup of the AM SCOPE 3.0MD 400 E digital microscope. There are designed to provide a magnified two-dimensional image that can be focused axially in successive focal planes.

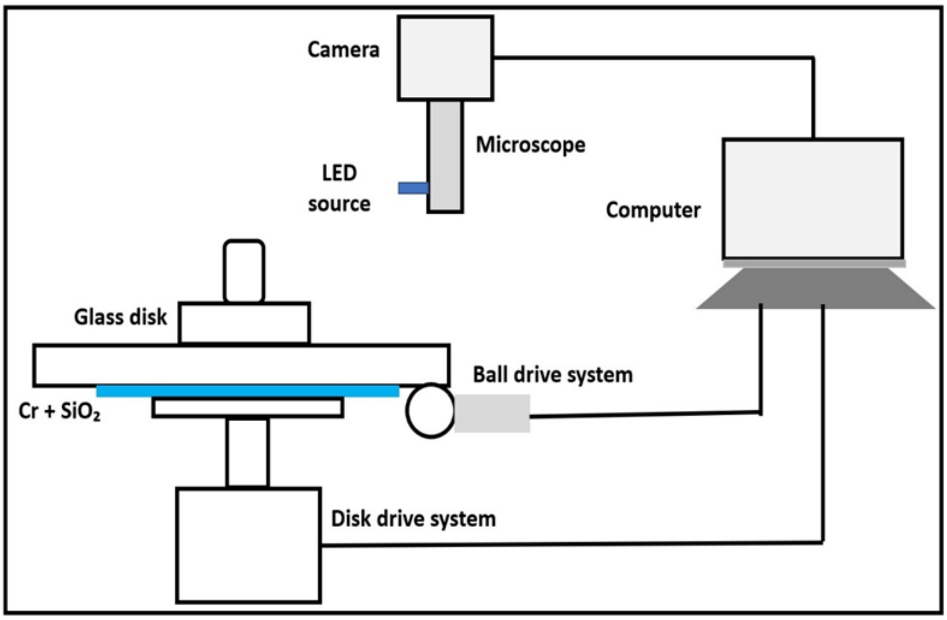

Figure 7: the microscope camera experimental setup of the AM SCOPE 3.0MD 400 E digital microscope.

4.0 Results and Discussion

The experimental setup forming the DELMS on mc-Si wafers is shown in the preceding section. We started with three different laser powers which are 15.2W, 23.5W, and 32.5W. The SEM images present (a) the front surface area with laser treatment, (b) a laser power of 15.2W, (c) a laser power of 23.5w, and (d) a laser power of 32.5W which are shown in figure 7. Only the areas with laser-treatment textures will etch at this stage, and we used KOH solution as our alkaline etchant, which is a pure inorganic solution.

The depth of DELMS increases as the laser power is higher. Clearly, the DELMS depth will continue to increase over time around a specific part of the wafer. At the same time, the exposed DELMS silicon wafer surface is continually etched by KOH solution during the etching process. This is due to KOH having a strong silicon oxide reaction selectivity, the depth achieved by laser power is high and becomes bigger. As a result, this self-controlled anisotropic etching will produce longitudinal micro-textures. The anisotropic etching creates a V-grooves pattern. From SEM data, the hole depth is 84.2μm with a laser power of 15.2W. This explains why the initial wafer thickness of 189.0 μm has around 55.0% remaining thickness.

Meanwhile, the depth of the hole created by 23.5W laser power is 104.3-µm. Since the laser power has increased, the thickness of the original wafer has decreased to roughly 48.0%. The deep etch is around 164.8-µm form after 32.5W laser power is treated on the front surface wafer. Table 2 shows the remaining Si thickness after the post-texturing process.

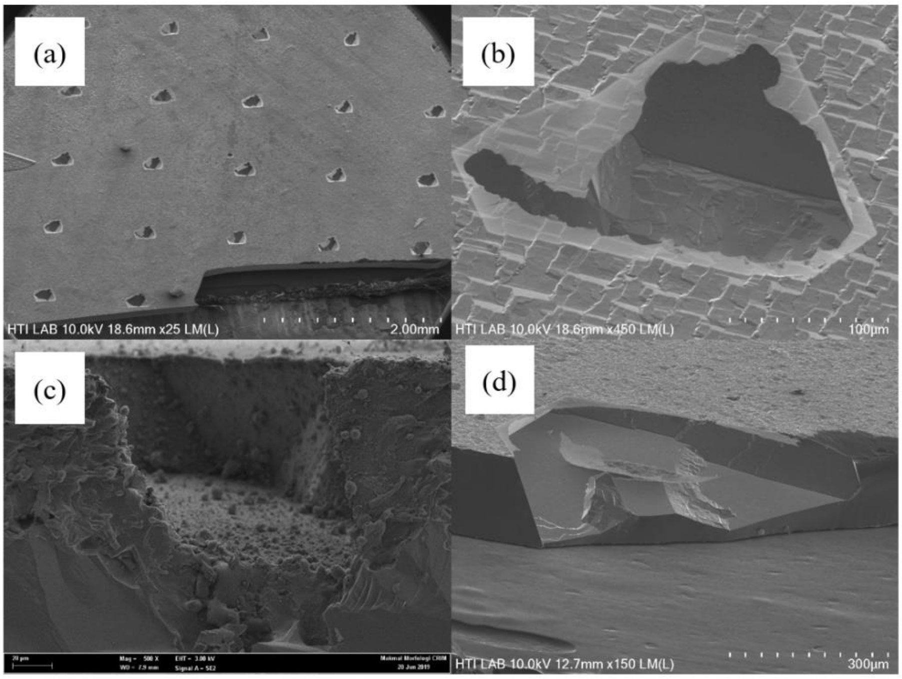

Figure 7: SEM images for polycrystalline Si wafers (a) top view of the wafer after laser texture treatment, laser power (b)15.2 W, (c) 23.5 W, and (d) 32.5 W.

Table 2: Nominated laser power and depth after a wet-chemical etching process

Sample with laser power in Watt(W)	Depth (µm)
15.2	84.20
23.5	104.34
32.5	164.80

We can clearly see from the SEM images that the laser treatment on the wafer surface has a significant influence and s highly reliant on laser power. The intensity of the laser beam on the wafer surface is increased due to the high laser power and low frequency (Rohaizar et al., 2019). Figure 7 (d) presents the rate of etching irregularly in partial hole patterns as a function of laser radiation and laser strength. A graph plotting recorded transmission data as a function of wavelength is shown in figure 8. Pyramid-textured polycrystalline transmission with a control sample of Si wafer has also been plotted. Due to numerous orders of magnitude changes in the sent signal, the transmission responses were shown on a log scale. The graph presents the transmission response of pyramid textured (no laser treatment) and samples with laser treatment at increasing laser power in the 900-nm to the 1000-nm spectral range.

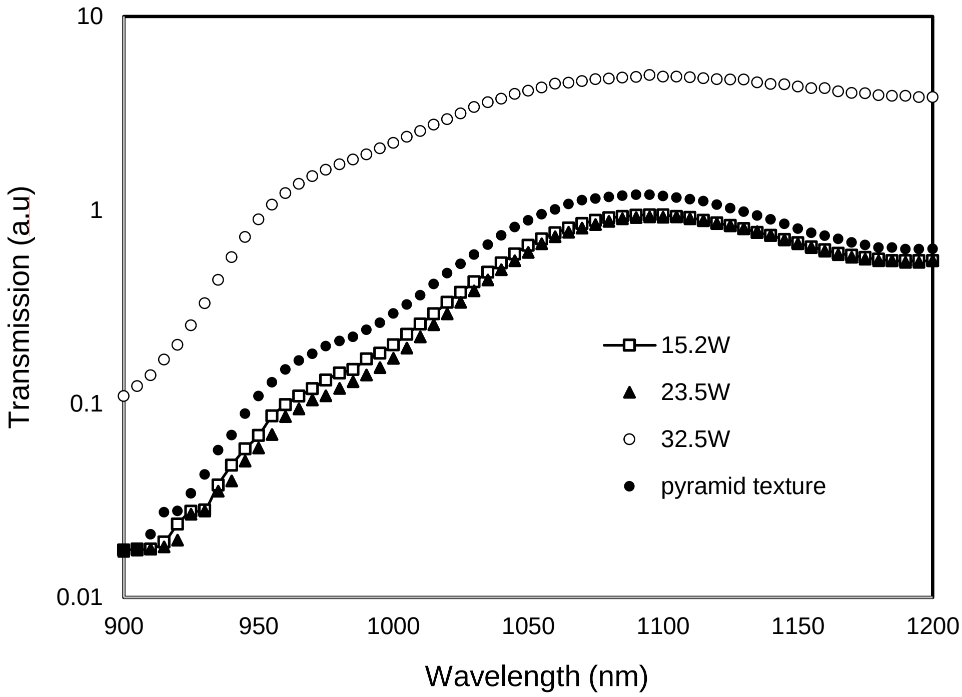

Figure 8: Optical measurement data as a function of wavelength; comparison measurement of 3-d laser textures by alkaline etch process with different laser fluences.

Due to the pyramid textured on the polycrystalline Si having a low transmission value. After texturing with KOH:IPA:H_2O, the pyramid texture appears with no additional anti-reflective coating texture. In comparison to the low power of 15.2W, the area with a high laser treatment of 32.5W has significantly higher transmission. The transmission through DELMS with a laser power of 15.2W is lower than a surface wafer with 23.5W between 1000 nm to 1100 nm. Furthermore, at a shorter wavelength (900 nm to 1000 nm), the pyramid texture exhibits higher transmission than the two-laser power (15.2W and 23.5W). We can observe that the laser texturing process produces a surface pattern and sidewall with certain roughness which is most likely the cause of increased light absorption.

This might be because of the depth after post-texturing, which results in a hole pattern. The DELMS features consist of pyramid texture on the left and right sidewall, as well as the flat area in the laser texture area, in this cell structure. Rohaizar et al. (2019) state that a lower-power laser creates its own texture due to quick melting and crystallization, which considerably improves internal scattering and results in increased absorption of light. Due to the hole pattern and high depth in texture, the sample with a laser power of 23.5W has the lowest transmission light. In comparison to 15.2W, this sample increased by 24.0% in depth. From this, it indicates that the optical path length in this laser area with 23.5W was higher which explains why light is absorbed more and transmits less. This presents that the laser texturing with 23.5W has qualities that strongly absorb more light, which is light bounced repeatedly more than the two times in DELMS design.

The transmission response shows the deepest depth in DELMS on the wafer surface, 32.5W laser power has the highest transmission compared to 15.2W and 23.5W. The light went through the silicon wafer without being scattered in this pattern, which is known as a partially-hole pattern. The DELMS area was quite thin compared with no DELMS area, therefore light is more transmitted than absorbed by the Si wafer due to the Si bandgap. Yilbas, Keles, & Toprakli, (2017) mention that a high laser power results in high intensity at the radiated spot edges and comparatively low intensity near the irradiated spot edges. The depth of the evaporated zona is modified as the irradiation spot edge approaches the center, generating a shallow depth known as a partially-hole pattern We can see from the IR transmission measurement analysis that the partially-hole pattern allows more light to flow through. This is owing to the leftover wafer thickness on a sample 32.5W laser power being around

In order to increase optical path length and absorption, it is typically vital for an effective solar cell that all the incident light can be scattered on the wafer surface (Nasir et al., 2016). The DELMS is a type of physical optic that works with deeply etched subwavelength patterns to form three-dimensional grating structures on the surface and through the substrate. In the etching solution, the principal reactive ions are the KOH/OH redox couple. The oxidation reaction removes a Si atom from the surface through a reaction with four OH ions (Zaidi, Ruby & Gee, 2001). The neutral $Si(OH)_4$ reacting diffuses into the solution away from the Si surface molecules. The four free electronWhere E_a = 0.595 eV, k_0 =2480 μm/h(mol/L)$^{-4.25}$ for (100) surface, and E_a =0.6 eV and k=4500 μm/h(mol/L)$^{-4.25}$ for (110) surface (Zaidi, Marquadt, Minhas & Tringe, 2002). Maximum Si etch is achieved for 10 % KOH concentration is 1.1 to1.5 μm/min at 70˚C to 75˚C temperature (Nasir et al., 2017).

The optical path length can be improved by designing a unique DELMS by changing the angle of incident of light which is commonly used to achieve light trapping. As a result, rather than being perpendicular to the surface, light travels at a different angle. Isabella et al. (2018) reported for enhancing the absorption of light, a commonly applied light management technique is the texturing of (internal) surfaces of the devices to scatter incident light away from the specular direction. In optics, we know that when light transversely through a weakly absorbing medium, electromagnet waves either visible light, ultraviolet, or infrared (IR), the transmission response is substantially reduced scattering off the surfaces. On the other hand, we observed the DELMS with laser power ranging from 15.2W to 32.5W, followed by post-texturing that formed on Si surfaces, increasing the light reaching the wafer surface and sidewall of the cell which had a long optical path length. The surface photovoltage (SPV) against wavelength for the sample with laser treatment of 23.5W is shown in figure 9.

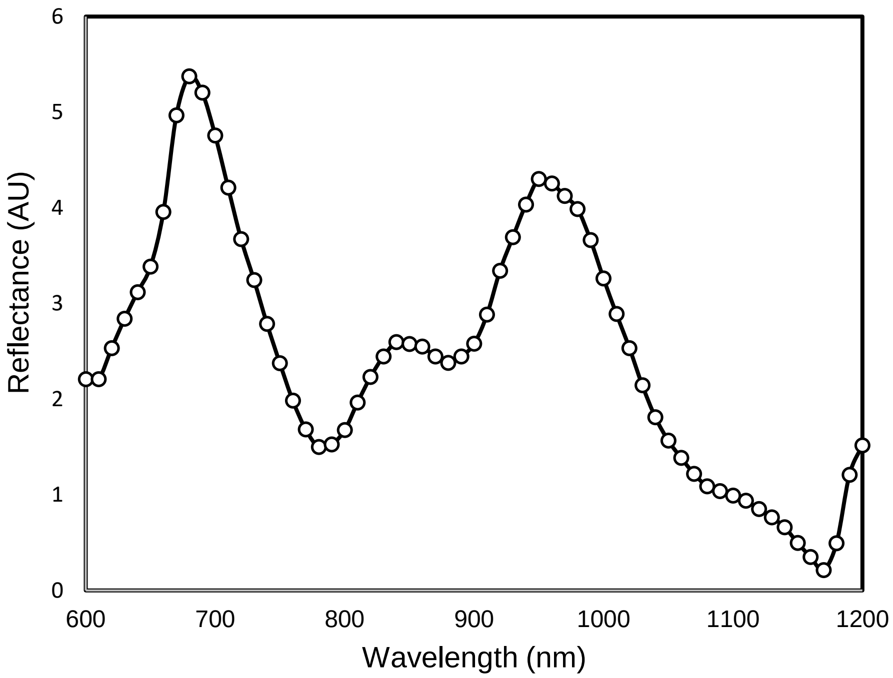

Figure.9: Surface Photovoltage versus wavelength for sample 23.5 W laser-treatment

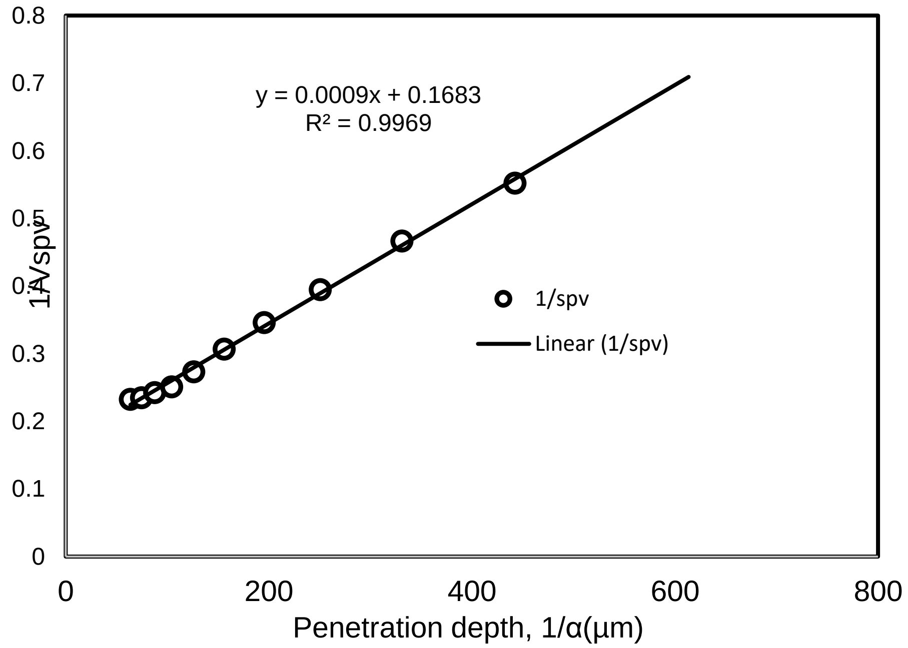

Figure 10: Graphical representation of 1/SPV versus penetration depth (1/α)

Wet-chemical texturization has a considerable impact on minority carrier lifetime and diffusion length. Minority carrier diffusion length was calculated using SPV data, with the largest peaks at 680nm, 850nm, and 980nm. The reciprocal of the silicon wafers' absorption coefficient (α) is the penetration depth (1/α). As illustrated in figure 10, the reciprocal of SPV data is plotted against the penetration depth (1/α) for diffusion length. We can observe from the graph that the best straight-line touches all of the data. The calculation can be made even more precise by adding more wavelengths. The diffusion length was determined using negative interception of the x-axis, which is 187.0-µm as shown in the graph. The minority carrier lifetime, L, and the minority carrier diffusivity of silicon, D are related by

$$L = \sqrt{D\tau} \qquad \text{... Equation 1}$$

The minority carrier lifetime sample of 23.5W laser treatment is 13.0-µs if the minority carrier diffusivity of silicon, D is 27.0cm²/s. The maximum carrier lifetime of crystalline Si solar cells must be 1milisecond, and the minority carrier diffusion length must be in the range of 100 to 300-µm (Akter et al., 2015). Basher et al, reported that the formation of uniform and homogeneous pyramidal morphology improved minority carrier lifetime and reduced recombination losses. Summarizes the averaged parameters of assembled cells (Basher, Hossain & Akand, 2018). These findings show that when compared to pyramid textured cells, the DELMS with 23.5W laser treatment has an 8.0% efficiency in 1.5cm×1.5cm size solar cells. The open-circuit voltage, V_{oc} is 1.8% lower than the pyramid texture (no laser treatment) and 11.0% lower than the commercial solar cells as in Table 3. Because of the rough surface textures and deep in-depth effects caused by laser treatment, the production of p-n junctions and front contact has become more difficult. We conclude that the texture's surface morphology has a significant impact on the patterns of solar cell performance. Due to a good light absorption increase, the DELMS on solar cells has a higher J_{sc} value than the pyramid textures (no laser treatment). In this study, we found that the relationship between V_{oc} and J_{sc} in an ideal planar p-n junction is given by the equation (Wolf, Descoeudres, Holman & Ballif, 2012)

$$V_{oc} = \frac{kT}{q} \ln\left(\frac{I_L}{I_0} + 1\right) \qquad \text{... Equation 2}$$

The Boltzmann constant is k, the temperature is Kelvin, the electron charge is q, and the dark saturation current is l_0. Equation 2 illustrated that the greater V_{oc} is when l is higher and l_0 is lower. The DELMS with 23.5W laser treatment has the greatest V_{oc} value, owing to their higher dark saturation current compared to the pyramid textures (no laser treatment) Si solar cells. Moreover, such recombination could be caused by a distorted p-n junction generated on the rough surface of a DELMS, which leads to increased junction leakage and dark saturation current. For pyramid textured, the average current density, J_{sc} is 24.0mA/cm². When compared to other cells with different laser treatment power energy, the J_{sc} for the cell with laser treatment of 23.5W has the highest J_{sc} value. The increased photon energy collecting by the DELMS is directly responsible for the increased value in J_{sc}. Furthermore, the J_{sc} of the DELMS with 23.5W increased by about 25.0% more than the pyramid texture polycrystalline Si as a control cell.

Table 3: Summary of parameter obtained by pyramid textured, 3-d laser texture structure and current-voltage measurement for 1cm²

Polycrystalline Si substrate	Laser power (W)	V_{oc} (V)	I_{sc} (mA)	J_{sc} (mA/cm^2)	FF (%)	η (%)
Conventional cell with Pyramid textured (no laser treatment)	-	0.493	24	24	42.26	5.00
3-dimensional laser textured	15.2	0.486	30	30	48.01	7.00
3-dimensional laser textured	23.5	0.484	36	36	45.91	8.00
3-dimensional laser textured	32.5	0.385	23	23	25.97	2.00
Commercial cell	-	0.546	23	23	55.74	7.00

Meanwhile, the optical performance of the DELMS for laser treatment 32.5W with widely spaced reflected and transmitting more light is inferior. Although the effect of laser treatment on cells minimizes light reflection, the cell's electrical function may be compromised. To enhance the light absorption gained by the DELMS, future research should consider superior surface passivation. We note that the DELMS fill factor, FF sample of 23.5W laser treatment is 45.91% greater than the pyramid texture (no laser treatment), which is 42.26%. The more effective charge carrier collection through the radial connection contributes to the FF increase of roughly 9.0%. As a result, the DELMS with 23.5W laser power increase the fraction of incident light traveling through the radial junction, resulting in a long light pathway in the DELMS 23.5W laser treatment polycrystalline Si solar cells outperformed all other cells, including the standard commercial.

The principal advantage of pyramid textures in a conventional polycrystalline (no laser treatment) on the wafer surface is that these textures reduce the amount of light reflected by the cell and give the highest V_{oc} value. However, this texture morphology is not suitable for maximizing a good light trapping mechanism without extra texture that enhances light traveling along with the cell structure. On a final note, we like to highlight the fact that by combining the pyramid textured, DELMS by laser pulsed, and post-texturing, we were able to realize solar cells with excellent light absorption ability (high l_L) and high FF value which represents a viable alternative to current fabrication techniques of efficient mc-Si solar cells

5.0 Conclusion

We offer a unique structure with periodic DELMS and post-texturing with an alkaline etching process, as well as a potential explanation of the fundamental mechanism underpinning These structures, using fewer materials, and the production of subwavelength arrays. Basically, for anti-reflecting silicon wafer production, we used a one-step wafer-scale micro-manufacturing process. As a result, the wafer-scale fabrication strategy is applicable to polycrystalline, monocrystalline, thin films, and even flexible substrates. We were able to demonstrate that the DELMS exhibit extraordinarily high incident light absorption over a wide wavelength range and at almost all angles of incidence. The DELMS design is very dependable, reproducible, and controllable, as well as exceeding time etched and cost-effective. Because these structure does not require any nanoparticle assembly to generate the light trapping or lithography process. The DELMS on a specific area of silicon surface can be faithfully generated in a few minutes, and varied depths will be present. The texture depth needs to be more or equal to 100 µm to avoid the formation of a thru-hole in the cell structure while keeping adequate light-trapping properties. We believe that this technology has the intrinsic capability to be integrated with normal silicon device fabrication. Given all the improvements over the present anti-reflecting scheme, it is obvious that the DELMS can be adapted by today's silicon solar cell to improve the high efficiency of silicon solar cells.

Acknowledgments
The authors would like to thank the Malaysia Ministry of Science Technology and Innovation (MOSTI) and Solar Energy Research Institute (SERI), National University of Malaysia, UKM for the financial support under the Science Fund Project with research code 03-01-02-SF13222 under consideration by another journal. All authors have played their roles to produce this research paper. All authors have approved and agreed to submit this final paper to this journal.

References

J. Baohua, "Nanophotonics Silicon Solar Cells: Status and Future Challenges," *Nanotechnol Rev*, vol. 4, no. 4, pp. 337–346, 2015, doi: 10.1515/ntrev-2015-0025

A. P. Amalathas and M. M.Alkaisi, "Nanostructures for Light Trapping in Thin Film Solar Cells," *Micromachine*, vol. 10, no. 9, p. 619, 2019, doi: 10.3390/mi10090619

X. Li and Y. Gua, "Theoritical fundamental of short pulse laser metal interaction: A review," *Nanotechnology and precision engineering*, vol. 3, no. 5, 2020, doi: 10.1016/j.npe.2020.08.001

Z. Q. Zhou, F. Hu, W.J. Zhou, H.Y.Chen, L.Ma, C.Zhang, and M. Lu. "An Investigation on a Crystalline-Silicon Solar Cell with Black Silicon Layer at the Rear," *Nanoscale Res Lett*, vol. 12, 2017, doi: 10.1186/s11671-017-2388-y.

Z. Liu, S.E. Sofia, H.S.Laine, M. woodhouse, S.Wieghold, I. M. Peters, and T. Buonassisi, "Revisiting Thin Silicon for Photovoltaic: A Technoeconomic Perspective ," *Energy Environment Science*, vol. 13, pp. 12–23, 2020, doi: 10.1039/C9EE02452B

A. R. Zanatta, “Revisiting the Optical Bandgap of Semiconductors and the Purposal of a unified methodology to its determination ,” *Sci Rep*, vol. 9, no. 1125, 2019.

J. Hüpkes, G. C. E. Jost, T. Merdzhanova, J. I. Owen, and T. Zimmermann, “Coupling and Trapping of Light in Thin-Film Solar Cells Using Modulated Interface Textures,” *Applied Sciences*, vol. 9, no. 21, p. 4648, Nov. 2019, doi: 10.3390/app9214648.

T. Jeewandara, “Absorption limit silicon short wavelength infrared,” *Phys.org*. 2020, doi: 10.1126/sciadu.abb0576

N Shanmugam, R. Pugazhendhi, R.M.Elavarasan, P. Kasiviswandthan, and N. Das, “Anti-reflective Coating Materials : A Holistic Review from PV Perspective,” *Energies (Basel)*, vol. 13, p. 2631, 2020.

L. Chen, Q. Wang, W. Chen, D. Liu, Z. Zhao, and D. Wang, “Light trapping mechanism of hemisphere cone arrays for silicon solar cells,” *Solar Energy*, vol. 163, pp. 519–525, Mar. 2018, doi: 10.1016/j.solener.2017.10.004.

F. A. H. Mutlak, A. F. Ahmed, U. M. Nayef, Q. Al-zaidi, and S. K. Abdulridha, “Improvement of absorption light of laser texturing on silicon surface for optoelectronic application,” *Optik (Stuttg)*, vol. 237, Jul. 2021, doi: 10.1016/j.ijleo.2021.166755.

S. A. Nadi, K.Bittkan, F. Lentz, K. Ding, and U.Rau, “Design of Determination Light-trapping Structure for Thin Silicon Heterojunction Solar Cells,” *Optic Express*, vol. 29, no. 5, pp. 7410–7417, 2021, doi: 10.1364/OE.417848

Ngwe Zin, “Recombination Free Reactive Ion Etch for High Efficiency Silicon Solar Cells,” *Solar ENergy Materials and Solar Cells*, vol. 172, pp. 55–58, 2017.

A. Otaegi, V. fano, M.A. Rasool, J.R. Gutierrez, J.C. Jimeno, N.Azkona, and E. Cereceda, “Progress in the Explaination and Modelling of the Laser-induced Damage of Edge-isolation Processes in Crystalline Silicon Solar Cells,” *Solar Energy*, vol. 155, pp. 847–853, 2017.

J. E. Park, W.S. Choi, J.J. Jang, E.J.Bae, and D.Lim, “Effect of Laser Doping on the Formation of the Selective Emitter of a c-Si Solar Cells,” *Appl. Sci*, vol. 10, no. 13, p. 4554, 2020.

J. Weber, S. Gutscher, S. Lohmüller, E. Lohmüller, and A. A. Brand, “Laser-Doped Selective Emitter-Process Development and Speed-Up.” In presented at the 35th European PV Solar Energy Conference and Exhibition 24-28 September 2018, Brussels, Belgium.

J. M. Y. Ali, V. Shanmugam, A.Kanna, P.Wang, N.balaji, R.V. Tabajonda, D.J. Perez, A.G.Aberle, and T. Mueller, "Analysis of nanosecond and femtosecond laser ablation of rear dielectrics of silicon wafer solar cells," *Solar Energy Materials and Solar Cells*, vol. 192, pp. 117–122, Apr. 2019, doi: 10.1016/j.solmat.2018.12.002.

B. S. Yilbas, O. Keles, and A. Y. Toprakli, "Surface Engineering towards Self-Cleaning Applications: Laser Textured Silicon Surface," in *Procedia Engineering*, 2017, vol. 184, pp. 716–724. doi: 10.1016/j.proeng.2017.04.147.

F. B. Radfar, F. Es, H.Nasser, O. Aldemir, A.Bele, and R Turan, "Effect of Laser Parameters and Post-texturing Treatment on the Optical and Electrical Properties of Laser Textured c-Si Wafers," in *AIP Conference Proceeding 1999*, 2018, p. 05008.

L. C. Andreani, A. Bozzola, P. Kowalczewski, M. Liscidini, and L. Redorici, "Silicon solar cells: Toward the efficiency limits," *Advances in Physics: X*, vol. 4, no. 1. Taylor and Francis Ltd., Jan. 01, 2019. doi: 10.1080/23746149.2018.1548305.

T. K. Chong, J Wilson, S. Mokkapati and K. Catchpole, "Optical Wavelngth Scale diffraction Gratings for light trapping in Solar cells," *J. Optik*, vol. 14, no. 2, p. 024012, 2012.

F. N. Ning, J. Mitchel, L. Zheng, J.Liu, C.Y.Hog, L.C.Kimerling, and X.Duan, "Design of Highly Efficient light-trapping structures for thin-film crystalline Si solar cell," *IEEE Trans Electron Dev*, vol. 54, no. 8, 2007, doi: 10.1109/TED.2007.900976

B. Radfar, F. Es, and R. Turan, "Effects of different laser modified surface morphologies and post-texturing cleanings on c-Si solar cell performance," *Renew Energy*, vol. 145, pp. 2707–2714, Jan. 2020, doi: 10.1016/j.renene.2019.08.031.

M. H. Rohaizar, S.Sepeai, N.Surhada, N.A.Ludin, M.A.Ibrahim, K.Sopian, and S.H.Zaidi, "Light transmission and internal scattering in pulsed laser-etched partially-transparent silicon wafers," *Heliyon*, vol. 5, no. 11, Nov. 2019, doi: 10.1016/j.heliyon.2019.e02790.

M. E. Fujishima D, Inoue H, Tsunomura Y, Asaumi T, Taira S, Kinishita T, Taguchi M, Sakata H, "High performance HITSolar cells for thinner S wafers," *2010 35th IEEE Photovoltaic Specialist Conference (PVSC)*, pp. 3137–3140, 2010.

C. J. Abott, "Optical and Electrical properties of Laser Texturing for High Efficiency Solar Cells," *Prog Photovoltaic Res Apll*, vol. 14, pp. 225–235, 2006.

J. Ding, S.Zou, J.Choi, J.Cui, D.Yuan, H.Su, C.Wu, J. Zhu, X.Ye, and X.Su, "A laser texturing study on multi-crystalline silicon solar cells," *Solar Energy Materials and Solar Cells*, vol. 214, Aug. 2020, doi: 10.1016/j.solmat.2020.110587.

H. S. Kim, S. H. Ha, S. J. Park, and J. H. Kim, "Effect of Surface Cleaning on Laser Texturing of Multicrystalline Silicon Wafer," *Sci Adv Mater*, vol. 10, no. 5, pp. 690–693, Jan. 2018, doi: 10.1166/sam.2018.3148.

Y. Zou, S.Li, W.Ma, Z.Ding, F.Yi, Y.Lie, and Z.Chan, "Research on surface nano-texturation and wet-chemical passivation of multi-crystalline silicon wafer," *Journal of Materials Science: Materials in Electronics*, vol. 28, no. 24, pp. 18825–18834, Dec. 2017, doi: 10.1007/s10854-017-7832-3.

L. A. Dobrzański and A. Drygała, "Surface texturing of multicrystalline silicon solar cells Manufacturing and processing," 2008.

N.S.M.Nasir, S.Sepeai, C.S.Leong, M.Y.Sulaiman, K.Sopian, and S.H.Zaidi, "Controllable Optical Transmission In Bifacial Silicon Solar Cells," *Solid State Science and Technology*, vol. 24, no. 1, pp. 127–138, 2016, ISSN 0128-7389 | http://journal.masshp.net 127

S. H. Zaidi, D. S. Ruby, and J. M. Gee, "Characterization of Random Reactive Ion Etched-Textured Silicon Solar Cells," vol. 48, no. 6, pp. 1200–1206, 2001.

S. H. Zaidi, R. Marquadt, B. Minhas, and J. W. Tringe, "Deeply etched grating structures for enhanced absorption in thin c-Si solar cells," *Conference Record of the Twenty-Ninth IEEE Photovoltaic Specialists Conference, 2002.*, pp. 1290–1293, 2002, doi: 10.1109/PVSC.2002.1190845.

N. S. M. Nasir, N. A. M. Sinin, S. Sepeai, C. S. Leong, K. Sopian, and S. H. Zaidi, "Investigation near IR absorption in thin crystalline Si wafers with randomly etched nano-pillars," in *AIP Conference Proceedings*, May 2017, vol. 1838. doi: 10.1063/1.4982177.

N.Akter, H.Zahid, Z.H.Mahmood, M.A. Tonima, M.Hoq, M. Abdur, R. akand, M.K.Basher, and M.Hanif., "Minority Carrier Diffusion Length by SPV Measurement for Calculation of Carrier Generation and Recombination of Silicon Solar Cells," in *ICMEIM*, 2015.

M. K. Basher, M. K. Hossain, and M. A. R. Akand, "Effect of surface texturization on minority carrier lifetime and photovoltaic performance of monocrystalline silicon solar cell," *Optik (Stuttg)*, vol. 176, pp. 93–101, Jan. 2019, doi: 10.1016/j.ijleo.2018.09.042.

S.D Wolf, A. Descoeudres, Z.C. Holman, and C.Ballif, "High-efficiency Silicon Heterojunction Solar Cells: A Review," *Green*, vol. 2, pp. 7–24, 2012.